

A divided spectrum balanced detection technique for intensity noise reduction in SAC OCDMA systems

Ahmed M. Alhassan ^{a,*}, Nasreen Badruddin ^a, N.M. Saad ^a, S.A. Aljunid ^b

^a Electrical and Electronics Engineering Department, Universiti Teknologi PETRONAS, Bandar Seri Iskandar, 31750 Tronoh, Perak, Malaysia

^b School of Computer and Communication Engineering, Universiti Malaysia Perlis, Malaysia

ARTICLE INFO

Article history:

Received 27 November 2012

Accepted 20 April 2013

Keywords:

Optical code division multiple access (OCDMA)

Spectral amplitude coding (SAC)

Phase induced intensity noise (PIIN)

Balanced detection

Divided spectrum balanced detection (DSBD)

ABSTRACT

In this paper we propose a simple divided spectrum balanced detection (DSBD) for spectral amplitude coding (SAC) optical code division multiple access (OCDMA) systems. SAC OCDMA systems are limited by phase induced intensity noise (PIIN), which is a signal dependent source of noise. Our proposed technique reduces the PIIN by dividing the spectrum of the signal into two or more, and detecting each spectrum by a different photodiode. The DSBD scheme reduces the detected optical power at photodetection, thus resulting in a higher mitigation of the PIIN. Theoretical results show that DSBD demonstrate noticeable improvement over traditional balanced detection technique, for example an up to 33% increase in the number of active users can be achieved, and at least 1×10^{-3} b/s Hz increase in the spectral efficiency is obtained. However, the DSBD is more complex and append more constrains on system components.

© 2013 Elsevier GmbH. All rights reserved.

1. Introduction

As the demand for high speed broadband services to the end users increases, the need for high speed access networks becomes more and more crucial. Different solutions have been proposed to provide high bandwidth to the customers [1,2]. But most of these solutions are too expensive to implement and require a change in the infrastructure. An attractive high bandwidth, low cost solution is to adopt optical code division multiple access (OCDMA) in access networks [3].

Of all OCDMA systems, spectral amplitude coding (SAC) OCDMA seems to be the most practical solution [4]. The main attractive feature of SAC OCDMA systems is their ability to cancel multi access interference (MAI) via a balanced detector at the receiver. Furthermore, these systems can use cheap light emitting diodes (LED) as sources due to their wide bandwidth, which is required in SAC encoding. However, in spite of their major advantages these sources are thermal in nature, and thus suffer from intensity noise (IN) [5].

Phase induced intensity noise (PIIN) or simply, intensity noise, is due to the square law of photodetection of thermal sources, and is considered the main limiting factor in SAC OCDMA systems [5]. Different methods have been proposed to counter PIIN in these systems. Since PIIN increases with the number of overlapping spectra, codes with ideal cross correlation value of one ($\lambda = 1$) have been

proposed in [6–8] to reduce the effect of PIIN. In [9], a hybrid wavelength division multiplexing (WDM) SAC OCDMA structure was considered by Yang to further reduce the number of spectral overlaps. Another method to reduce the number of spectral overlaps was proposed by Yang et al. by including the spatial domain into the code space [10,11]. In [12], Pennon et al. developed a numerical optimized method for fiber Bragg grating (FBG) frequency response to maximize the available capacity in the presence of both PIIN and MAI. A noise cleaning approach which used saturated semiconductor optical amplifiers (SOA) to reduce the PIIN was first investigated by McCoy et al. for SAC OCDMA systems [13]. They concluded that these systems suffer from post filtering effect that limits the PIIN reduction. Pennon et al. [14] introduced notch filters in one of the arms of receiver balanced detector to abate the post filtering effect. In [15], a multi-photodiode balanced detection (MPBD) was proposed to reduce PIIN via reduction of power at the photodetectors. Since the PIIN is proportional to the square of the power of the received signal, by reducing the received power at the photodiode this reduces the PIIN. The optical signal was split and fed into multiple photodiodes to achieve both reduction in the PIIN and to maintain the same average photocurrent.

However, in [15] the two split signal was assumed to be independent, which is not entirely true. Abtahi et al. [16], showed that a high degree of correlation will always exist between two signals generated from the same source and have the same optical spectrum. Thus the results given in [15] are highly optimistic and at best can be considered as the absolute upper limit in performance enhancement using power reduction.

* Corresponding author.

E-mail address: ahmed7060@yahoo.com (A.M. Alhassan).

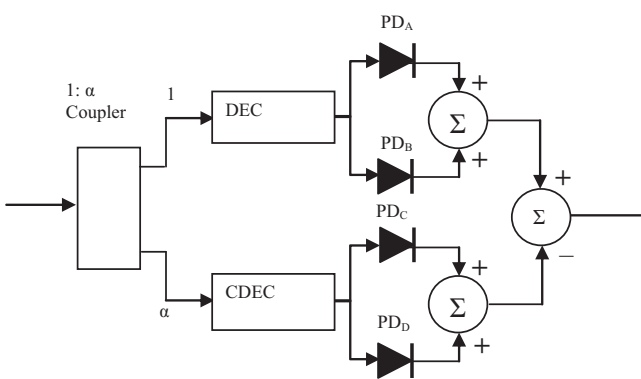


Fig. 1. Structure of the multi-photodiode balanced detection. DEC: decoder; CDEC: complementary decoder; PD: photodiode.

In this paper, we consider the same idea as in [15], but instead of splitting the signal based on power, we split (or filter) the spectrum of the received optical signal. When we split the spectrum we can achieve two major goals; firstly, we reduce the power received at each photodiode which directly reduces the PIIN. Secondly, the two split signals can be considered independent as they come from two different spectra [16], and thus higher performance improvements can be obtained.

The rest of this paper is divided as follows: in Section 2, we discuss the limitations of the MPBD. In Section 3, we propose a divided spectrum balanced detection technique that reduces the PIIN, and we generate the performance equations for our proposed technique. We show and discuss the results obtained in Section 4. Finally, a conclusion that highlights the major benefits and limitations of the proposed scheme is given in Section 5.

2. Multi-photodiode balanced detection

The structure of the MPBD technique with four photodiodes is shown in Fig. 1. The received optical signal is split into two signals by the $1:\alpha$ optical coupler, where the value of α depends on the code family and the code weight. The upper signal is decoded by a decoder (which has the same spectral distribution as the desired user's encoder), and the lower arm signal is decoded by a complementary decoder (which has a spectral distribution that is complementary to desired user's encoder). The decoded signals on both branches are split again into two equal signals using 3-dB splitters. After photodetection, the electrical signals from photodiodes PD_A and PD_B (the decoder branch) are summed up, and the electrical signal from photodiodes PD_C and PD_D (the complementary decoder branch) are summed up. To extract the desired user's information and cancel the first order (mean) MAI, the complementary decoder branch signal is subtracted from the decoder branch signal.

In order for the MPBD to reduce the PIIN, the two signals in upper branch (and the lower branch) must be independent. However, since these two signals have the same optical spectrum, then we cannot consider them as independent [16]. The two split signals will be highly correlated and the degree of PIIN reduction will be much less than the results given in [15].

3. Divided spectrum balanced detection (DSBD)

3.1. The structure of the DSBD scheme

To reduce the power at photodetection and at the same time achieve independence between the two signals, we propose to split or divide the signal into two or more different spectra. Fig. 2

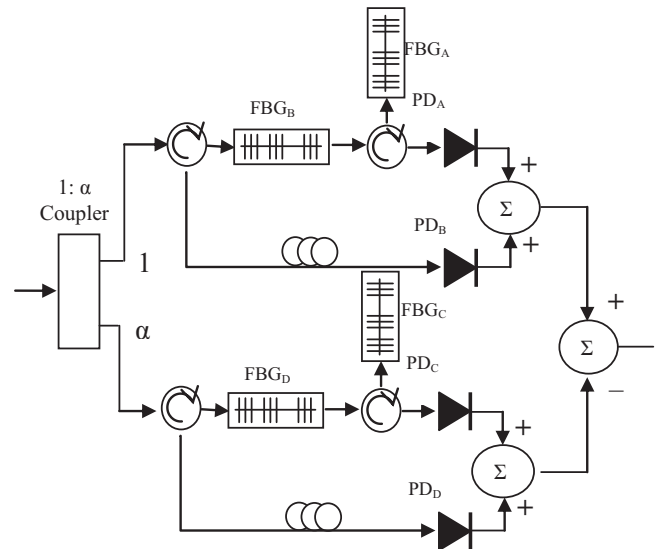


Fig. 2. Structure of DSBD receiver. FBG: fiber Bragg grating.

shows the divided spectrum balanced detection (DSBD) systems that uses four photodiodes. At the upper arm (the decoder), the optical signal is passed to a fiber Bragg grating (FBG) in reflection (other filter technologies [6,14,17] can be used, but receiver structure will have some minor changes) FBG_B . The FBG_B will reflect half of the desired user spectrum and any overlapping interferers chip within that spectrum to photodiode PD_B . The remaining spectra are passed to FBG_A which reflect the other half of the desired user spectrum and any other overlapping chip within that spectrum to photodiode PD_A . The same general principle is applied at the lower arm (the complementary decoder), where approximately half of the remaining spectra (not including the spectrum in filtered out by FBG_A and FBG_B) are passed to PD_C by FBG_C and the rest of the spectra is directed to photodiode PD_D via FBG_D .

By dividing the spectrum of decoded and the complementary decoded signals into two or more, we can achieve both the reduction in power and most importantly the independence between the split signals, which results in a higher mitigation of the PIIN.

3.2. Performance analysis of the DSBD

We follow the same procedure in our analysis as in [18]. To simplify our performance analysis, firstly we assume that the power reaching the receiver is high enough (>-20 dBm) so only the intensity noise is taken into consideration.

Secondly, for the decoder branch, we will assume that half of the desired users weight ($p+1$ for modified quadratic congruence (MQC) codes [6], where p is the prime number) is filtered out by FBG_B and the other half is filtered out by FBG_A .

For the interferers, we assume that half of the interferers will have a single wavelength chip (a "1" chip) that coincide with one wavelength in FBG_B and the other half of the interferers will have single wavelength that will fall in FBG_A spectrum. Thus, for N_I interferer we can say:

$$N_A = \left\lceil \frac{N_I}{2} \right\rceil, \quad N_B = \left\lfloor \frac{N_I}{2} \right\rfloor \quad \text{where} \quad N_A + N_B = N_I \quad (1)$$

where N_A and N_B are the number of interferers that have shared spectrum pins with decoder FBG_A and FBG_B , respectively, and $\lceil x \rceil$ is the ceiling function of x , and $\lfloor x \rfloor$ is the floor function of x .

Thirdly, at the complementary decoder branch, each interferer has p spectral pins each with amplitude of α . We assume that these

p spectral pins are equally distributed between FBG_C and FBG_D . This can be expressed as:

$$N_I w_{FBG_C} + N_I w_{FBG_D} = p N_I \quad (2)$$

where $w_{FBG_C} = \left\lceil \frac{p}{2} \right\rceil$, and $w_{FBG_D} = \left\lfloor \frac{p}{2} \right\rfloor$

Thus, all the interferers (N_I) will be present at PD_C and PD_D , but with half the weight compared to BD scheme.

To compute the performance of our system, firstly, we need to derive the expressions for the power spectral density (PSD) at all four photodiodes for both cases when the desired user is active (sending data "1") or inactive (sending data "0").

For PD_A :

$$G_{A_0}(\nu) = p_0 \sum_{i=1}^{N_A} X_i(\nu) H_{DEC_A}(\nu) \quad (3)$$

$$G_{A_1}(\nu) = p_0 \left[H_E(\nu) H_{DEC_A}(\nu) + \sum_{i=1}^{N_A} X_i(\nu) H_{DEC_A}(\nu) \right] \quad (4)$$

and for PD_B

$$G_{B_0}(\nu) = p_0 \sum_{i=1}^{N_B} X_i(\nu) H_{DEC_B}(\nu) \quad (5)$$

$$G_{B_1}(\nu) = p_0 \left[H_E(\nu) H_{DEC_B}(\nu) + \sum_{i=1}^{N_B} X_i(\nu) H_{DEC_B}(\nu) \right] \quad (6)$$

for PD_C

$$G_{C_0}(\nu) = \alpha p_0 \sum_{i=1}^{N_I} X_i(\nu) H_{CD_C}(\nu) \quad (7)$$

$$G_{C_1}(\nu) = \alpha p_0 \left[H_E(\nu) H_{CD_C}(\nu) + \sum_{i=1}^{N_I} X_i(\nu) H_{CD_C}(\nu) \right] \quad (8)$$

and for PD_D

$$G_{D_0}(\nu) = \alpha p_0 \sum_{i=1}^{N_I} X_i(\nu) H_{CD_D}(\nu) \quad (9)$$

$$G_{D_1}(\nu) = \alpha p_0 \left[H_E(\nu) H_{CD_D}(\nu) + \sum_{i=1}^{N_I} X_i(\nu) H_{CD_D}(\nu) \right] \quad (10)$$

where $G_{X_0}(\nu)$ and $G_{X_1}(\nu)$ are the PSDs for the photodiodes when the desired user is active or inactive, respectively, where PD_X represents a specific photodiode with $X \in \{A, B, C, D\}$. The power level of the PSD of the received signal is p_0 . $X_i(\nu)$ denotes the encoder transfer function of the i th arbitrary interferer. $H_{DEC_Y}(\nu)$ represents the decoder transfer function for the specific branch $Y \in \{A, B\}$, $H_{CD_Z}(\nu)$ denotes the complementary decoder transfer function for branch $Z \in \{C, D\}$, and $H_E(\nu)$ represents the encoders transfer function. Where the transfer function have the following relation:

$$H_{DEC_A} + H_{DEC_B} = H_{DEC} \quad (11)$$

and

$$H_{CD_C} + H_{CD_D} = H_{CD} \quad (12)$$

where H_{DEC} and H_{CD} are the decoder's and complementary decoder's transfer functions. The parameter α is the attenuator transmission factor on the complementary decoder side, and its

value is chosen to equalize the power between the decoder and the complementary decoder signals in the case of inactive user.

Next, we find the mean optical power

$$\bar{P} = \int_0^{B_o} G(\nu) d\nu \quad (13)$$

where B_o is the optical bandwidth on the source. The mean optical power reaching PD_A is given by:

$$\overline{P_{A_0}} = p_0 \sum_{i=1}^{N_A} \int_0^{B_o} X_i(\nu) H_{DEC_A}(\nu) d\nu \quad (14)$$

$$\overline{P_{A_1}} = p_0 \left[\int_0^{B_o} H_E(\nu) H_{DEC_A}(\nu) d\nu + \sum_{i=1}^{N_A} \int_0^{B_o} X_i(\nu) H_{DEC_A}(\nu) d\nu \right] \quad (15)$$

A similar set of equations can be derived for $\overline{P_{B_0}}$ and $\overline{P_{B_1}}$ by making the proper substitutions of corresponding parameters.

For the complementary decoder branch, the mean power reaching PD_C is:

$$\overline{P_{C_0}} = \alpha p_0 \sum_{i=1}^{N_I} \int_0^{B_o} X_i(\nu) H_{CD_C}(\nu) d\nu \quad (16)$$

$$\overline{P_{C_1}} = \alpha p_0 \left[\int_0^{B_o} H_E(\nu) H_{CD_C}(\nu) d\nu + \sum_{i=1}^{N_I} \int_0^{B_o} X_i(\nu) H_{CD_C}(\nu) d\nu \right] \quad (17)$$

Similarly, equations for $\overline{P_{D_0}}$ and $\overline{P_{D_1}}$ can be derived.

From the general properties of SAC OCDMA codes we know that the cross correlation for all codes with the desired user is constant at both the decoder and complementary decoder [6], thus we can replace $X_i(\nu)$ with $X_I(\nu)$ which represents any arbitrary interferer.

At the decoder, we assume that N_A interferers are present at PD_A and N_B interferer are present at PD_B .

Thus, for the PD_A :

$$\overline{P_{A_0}} = p_0 N_A \int_0^{B_o} X_I(\nu) H_{DEC_A}(\nu) d\nu \quad (18)$$

$$\overline{P_{A_1}} = p_0 \left[\int_0^{B_o} H_E(\nu) H_{DEC_A}(\nu) d\nu + N_A \int_0^{B_o} X_I(\nu) H_{DEC_A}(\nu) d\nu \right] \quad (19)$$

Similar equations can be derived for PD_B

At the complementary decoder branch, all the interferers are present at both PD_C and PD_D .

Thus, for the PD_C :

$$\overline{P_{C_0}} = \alpha p_0 N_I \int_0^{B_o} X_I(\nu) H_{CD_C}(\nu) d\nu \quad (20)$$

$$\overline{P_{C_1}} = \alpha p_0 \left[\int_0^{B_o} H_E(\nu) H_{CD_C}(\nu) d\nu + N_C \int_0^{B_o} X_I(\nu) H_{CD_C}(\nu) d\nu \right] \quad (21)$$

The corresponding equations for PD_D can be similarly derived.

The mean optical power after detection is given by:

$$\begin{aligned} \bar{P} &= \overline{P_{A_1}} + \overline{P_{B_1}} - (\overline{P_{C_1}} + \overline{P_{D_1}}) \\ &= p_0 \int_0^{B_o} H_E(v)(H_{DEC_A}(v) + H_{DEC_B}(v)) dv \\ &\quad - \alpha p_0 \int_0^{B_o} H_E(v)(H_{CD_C}(v) + H_{CD_D}(v)) dv \\ &= p_0 \int_0^{B_o} H_E(v)(H_{DEC}(v) - \alpha H_{CD}(v)) dv \\ &= \overline{P_{DEC_1}} - \overline{P_{CD_1}} \end{aligned} \quad (22)$$

which is the same average power detected by the conventional balanced detector [18].

Next, we turn our attention to intensity noise computation. Assuming that the optical bandwidth is much larger than the electrical bandwidth (B_e), the PIIN for unpolarized thermal light is given by [5]:

$$\sigma^2 = B_e \int_0^{B_o} [G(v)]^2 dv \quad (23)$$

By observing (23), since $G(v)$ is dependent of the active number of interferers, the PIIN is going to conditional on the active number of interferers at each photodiode. Using (23) we calculate the PIIN for each photodiode.

The PIIN at PD_A in the case of data “0” and data “1” is given by:

$$\sigma_{P_{A_0}|N_A}^2 = \sum_{i=1}^{N_A} \sigma_{P_{A_i}}^2 + \sum_{i=1}^{N_A} \sum_{j=1, j \neq i}^{N_A} \sigma_{P_{A_ij}}^2 \quad (24)$$

and for data “1”, the PIIN is:

$$\sigma_{P_{A_1}|N_A}^2 = \sigma_{P_{A_E}}^2 + 2 \sum_{i=1}^{N_A} \sigma_{P_{A_iE}}^2 + \sum_{i=1}^{N_A} \sigma_{P_{A_i}}^2 + \sum_{i=1}^{N_A} \sum_{j=1, j \neq i}^{N_A} \sigma_{P_{A_ij}}^2 \quad (25)$$

where $\sigma_{P_{A_i}}^2$ is the beat noise from the interferer alone, and it is given by:

$$\sigma_{P_{A_i}}^2 = p_0^2 B_e \int_0^{B_o} (X_i(v) H_{DEC_A}(v))^2 dv \quad (26)$$

The beat noise from any two interferers beating together, $\sigma_{P_{A_ij}}^2$, is given as:

$$\sigma_{P_{A_ij}}^2 = p_0^2 B_e \int_0^{B_o} X_i(v) X_j(v) (H_{DEC_A}(v))^2 dv \quad (27)$$

and $\sigma_{P_{A_E}}^2$ is the intended users beating alone:

$$\sigma_{P_{A_E}}^2 = p_0^2 B_e \int_0^{B_o} (H_E(v) H_{DEC_A}(v))^2 dv \quad (28)$$

The beat generated by the desired users and an interferer beating together, $\sigma_{P_{A_iE}}^2$, is given as:

$$\sigma_{P_{A_iE}}^2 = p_0^2 B_e \int_0^{B_o} X_i(v) H_E(v) (H_{DEC_A}(v))^2 dv \quad (29)$$

Similar computations are required for the PD_B and for complementary decoder photodiodes PD_C and PD_D .

The optical noise equations can be simplified by applying the general principles of any SAC OCDMA code [6] to get:

$$\sigma_{P_{A_0}|N_I}^2 = N_A \sigma_{P_{A_I}}^2 + N_A (N_A - 1) \overline{\sigma_{P_{A_ij}}^2} \quad (30)$$

and

$$\sigma_{P_{A_1}|N_I}^2 = \sigma_{P_{A_E}}^2 + 2N_A \sigma_{P_{A_iE}}^2 + N_A \sigma_{P_{A_I}}^2 + N_A (N_A - 1) \overline{\sigma_{P_{A_ij}}^2} \quad (31)$$

where the subscript I represents any arbitrary interferer, and $\overline{\sigma_{P_{A_ij}}^2}$ designates the average PIIN over all code pairs for the spectrum covered by FBG_A . Similar equations are also derived for $\sigma_{P_{B_0}|N_B}^2$, $\sigma_{P_{B_1}|N_B}^2$, $\sigma_{P_{C_0}|N_I}^2$, $\sigma_{P_{C_1}|N_I}^2$, $\sigma_{P_{D_0}|N_I}^2$ and $\sigma_{P_{D_1}|N_I}^2$.

Using the calculated mean optical power and the optical noise from the previously derived equations, we compute the probability density function (pdf) for each photodiode.

The pdf can be approximated by a Gamma distribution [19]:

$$f_P(P) = \left(\frac{SNR}{\bar{P}} \right)^{SNR} \frac{P^{SNR-1}}{\Gamma(SNR)} \exp \left(-SNR \frac{P}{\bar{P}} \right) \quad (32)$$

where \bar{P} is the mean optical power, Γ is the Gamma function and the SNR is the signal to noise ratio and its given by:

$$SNR = \frac{\bar{P}^2}{\sigma^2} \quad (33)$$

The pdfs for all photodiodes for both cases for data “0” and “1” must be calculated using the expressions for the mean power and optical noises derived previously.

For the decoder branch, the electrical signals from photodiodes PD_A and PD_B are added. Since the PSDs on photodiode PD_A and PD_B originate from different spectrums, then it is safe to assume that the signals are independent [16].

Thus, the resultant pdf is the convolution of pdf PD_A and pdf PD_B . The same applies to the complementary decoder branches PD_C and PD_D .

$$f_{P_{DEC_0}|N_I}(P_{DEC_0}|N_I) = f_{P_{A_0}|N_A}(P_{A_0}|N_A) * f_{P_{B_0}|N_B}(P_{B_0}|N_B) \quad (34)$$

$$f_{P_{CD_0}|N_I}(P_{CD_0}|N_I) = f_{P_{C_0}|N_I}(P_{C_0}|N_I) * f_{P_{D_0}|N_I}(P_{D_0}|N_I) \quad (35)$$

where $f_{P_{DEC_0}|N_I}(P_{DEC_0}|N_I)$ and $f_{P_{CD_0}|N_I}(P_{CD_0}|N_I)$ are the pdfs for the decoder and the complementary decoder for data “0”, respectively. The pdfs for data “1” $f_{P_{DEC_1}|N_I}(P_{DEC_1}|N_I)$ and $f_{P_{CD_1}|N_I}(P_{CD_1}|N_I)$ are computed in a similar way.

To extract the desired user signal and cancel MAI, the two signals coming from the decoder and the complementary decoder are subtracted from each other. This is equivalent to the correlation of the respective pdfs.

$$f_{P_0|N_I}(P_0|N_I) = f_{P_{D_0}|N_I}(P_{D_0}|N_I) \otimes f_{P_{CD_0}|N_I}(P_{CD_0}|N_I) \quad (36)$$

and

$$f_{P_1|N_I}(P_1|N_I) = f_{P_{D_1}|N_I}(P_{D_1}|N_I) \otimes f_{P_{CD_1}|N_I}(P_{CD_1}|N_I) \quad (37)$$

Using the two conditional density functions in (36) and (37) and assuming that the active number of users, N_I obeys a binomial distribution, the bit error rate (BER) for DSBD is given by:

$$\begin{aligned} BER &= \frac{1}{2} \sum_{N_I=0}^{N-1} 0.5^{N-1} \frac{(N-1)!}{N_I!(N-N_I-1)!} \\ &\quad \times \left[\int_{\gamma}^{\infty} f_{P_0|N_I}(P_0|N_I) + \int_{-\infty}^{\gamma} f_{P_1|N_I}(P_1|N_I) \right] \end{aligned} \quad (38)$$

where N is the total number of users and γ is the optical power threshold value to distinguish between data level “0” and data level “1”.

Another performance metric that we use to compare the DSBD with the BD is the spectral efficiency. The spectral efficiency is defined as the total system throughput per unit optical bandwidth for a specific BER, and can be expressed as:

$$SE = \frac{N_I R}{B_o} \quad (39)$$

where R is the data rate.

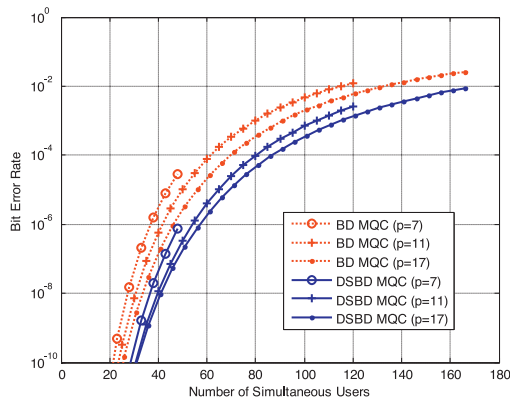


Fig. 3. BER versus active number of users for MQC ($p = 7, 11$ and 17) codes, at data rate 622 Mb/s and optical bandwidth 30 nm .

The electrical bandwidth is chosen to be 75% of the data rate (for fourth order Bessel Thompson filter), thus SE can be expressed as:

$$SE = \frac{4N_I B_e}{3B_o} \quad (40)$$

4. Results and discussions

Using the BER equations generated in the previous section, we evaluate the performance of our proposed system. We assume that all the electrical and optical filters have a rectangular shape, and that the light is unpolarized incoherent light. The system under evaluation is unipolar system, that is, no light is sent to represent data “0” while a pulse of light is sent to indicate data “1”.

The BER against the active number of simultaneous users is given in Fig. 3 for different MQC codes. The data rate is 622 Mb/s , and the electrical bandwidth is taken to be 75% of the data rate. For a 30 nm optical bandwidth, Fig. 3 clearly shows a noticeable improvement for the DSBD over the traditional BD for all given prime number (7, 11 and 17). For example, considering error free transmission ($\text{BER} = 10^{-9}$), and for prime number ($p = 17$), the percentage improvement in the number of simultaneous active users is approximately 17%.

A comparison between the proposed DSBD and the BD schemes for different data rates is shown in Figs. 4 and 5 for an optical bandwidth of 10 nm and 30 nm , respectively. The prime number value is 13, and the electrical bandwidth is 75% of the data rate. The curves for the BD scheme for the different data rates coincide smoothly with results given in [20] which confirm the accuracy of our calculations. From Figs. 4 and 5, we can see that the MPBD outperforms

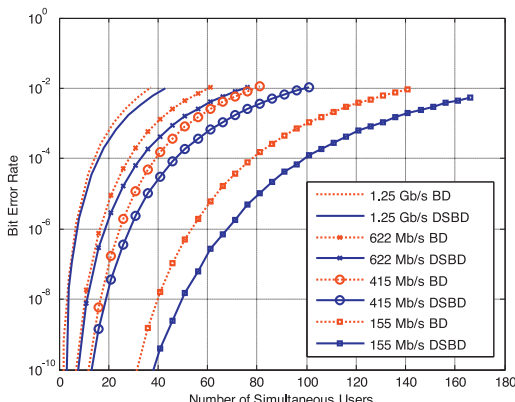


Fig. 4. BER versus active number of users for MQC code ($p = 13$), at different data rate with optical bandwidth 10 nm .

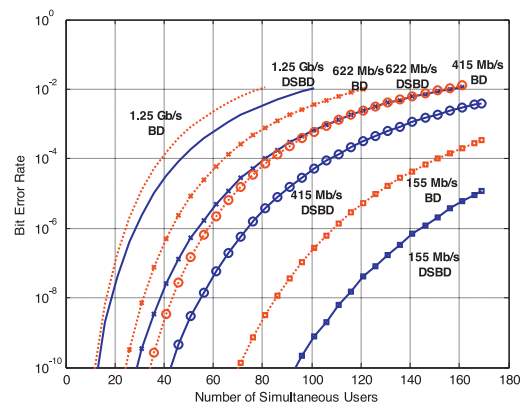


Fig. 5. BER versus active number of users for MQC code ($p = 13$), at different data rate with optical bandwidth 30 nm .

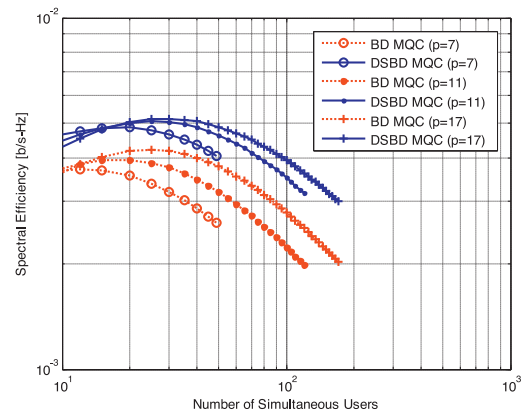


Fig. 6. Spectral efficiency versus the number of active users for the MQC code for different prime numbers at a $\text{BER} = 10^{-10}$.

the BD for all given data rates. For a data rate of 155 Mb/s and considering error free transmission, the percentage improvement in the simultaneous users is 28% and 33% for an optical bandwidth of 10 nm and 30 nm , respectively. As can be seen from Figs. 4 and 5, the percentage of improvement in the number of simultaneous active users is not constant, but is a function of both the optical and the electrical bandwidth.

The spectral efficiency (b/s Hz) versus the number of simultaneous users is given in Fig. 6. The ratio B_o/B_e is changed in the noise equations for all number of interferers (N_I) until the $\text{BER} = 10^{-10}$ (this BER is chosen for the sake of comparison with results in [18]). Using N_I and the ratio B_o/B_e , the spectral efficiency is calculated using (40). For a MQC code with prime number $p = 7$ the optimal spectral efficiencies for both the BD and DSBD are $3.7 \times 10^{-3} \text{ b/s Hz}$ and $4.7 \times 10^{-3} \text{ b/s Hz}$, respectively, and for a code with $p = 11$ the optimal spectral efficiencies for the BD and DSBD are $3.9 \times 10^{-3} \text{ b/s Hz}$ and $5.0 \times 10^{-3} \text{ b/s Hz}$, respectively, and for a code with $p = 17$ the optimal spectral efficiencies for the BD and DSBD are $4.2 \times 10^{-3} \text{ b/s Hz}$ and $5.2 \times 10^{-3} \text{ b/s Hz}$, respectively. As can be seen there is at least a 0.001 b/s Hz improvement in the spectral deficiency.

5. Conclusion

In this paper we proposed a simple divided spectrum balanced detection scheme to mitigate intensity noise in SAC OCDMA systems. Our proposed technique is based on splitting the spectrum of the received optical signal into two or more different spectra and detecting each spectrum by a different photodiode. This

approach achieves a reduction in the detected power which reduces the PIIN. Results show that the introduced method shows superior performance than the conventional balanced detection scheme. An improvement of up to 33% in the active number of users is obtained and an increase of up to 1.2×10^{-3} b/s Hz in the spectral efficiency is reported. On the other hand, the proposed system is more complex, and requires that the system components (e.g. photodiodes) be well matched.

References

- [1] R. Feldman, E. Harstead, S. Jiang, T. Wood, M. Zirngibl, An evaluation of architectures incorporating wavelength division multiplexing for broad-band fiber access, *J. Lightw. Technol.* 16 (September (9)) (1998) 1546–1559.
- [2] J. Prat, C. Arellano, V. Polo, C. Bock, Optical network unit based on a bidirectional reflective semiconductor optical amplifier for fiber-to-the-home networks, *IEEE Photon. Technol. Lett.* 18 (January (1)) (2005) 250–252.
- [3] P.R. Prucnal, *Optical Code Division Multiple Access: Fundamentals and Applications*, Taylor & Francis, New York, 2005.
- [4] D. Zaccarin, M. Kavehrad, An optical CDMA system based on spectral encoding of LED, *IEEE Photon. Technol. Lett.* 4 (April) (1993) 479–482.
- [5] E.D.J. Smith, R.J. Blaikie, D.P. Taylor, Performance enhancement of spectral-amplitude-coding optical CDMA using pulse-position modulation, *IEEE Trans. Commun.* 46 (September (9)) (1998) 1176–1185.
- [6] Z. Wei, H.M.H. Shalaby, H. Ghafouri-Shiraz, Modified quadratic congruence codes for fiber Bragg-grating-based spectral-amplitude coding optical CDMA systems, *J. Lightw. Technol.* 19 (September (9)) (2001) 1274–1281.
- [7] Z. Wei, H. Ghafouri-Shiraz, Codes for spectral-amplitude-coding optical CDMA systems, *J. Lightw. Technol.* 50 (August (8)) (2002) 1209–1212.
- [8] S.A. Aljunid, M. Ismail, A.R. Ramli, M.A. Borhanuddin, M.K. Abdullah, A new family of optical code sequences for spectral-amplitude-coding optical CDMA systems, *IEEE Photon. Technol. Lett.* 16 (October (10)) (2004).
- [9] C.C. Yang, Hybrid wavelength-division-multiplexing/spectral-amplitude-coding optical CDMA system, *IEEE Photon. Technol. Lett.* 17 (June (6)) (2005) 1343–1345.
- [10] C.C. Yang, J.F. Huang, Two-dimensional M-matrices coding in spatial/frequency optical CDMA networks, *IEEE Photon. Technol. Lett.* 15 (January (1)) (2003) 168–170.
- [11] J.F. Huang, C.C. Yang, Permuted M-matrices for the reduction of phase-induced intensity noise in optical CDMA network, *IEEE Trans. Commun.* 54 (June (1)) (2006) 150–158.
- [12] J. Penon, Z.A. El-Sahn, L.A. Rusch, S. LaRochelle, Spectral-amplitude-coded OCDMA optimized for a realistic FBG frequency response, *J. Lightw. Technol.* 25 (May (5)) (2007) 1256–1263.
- [13] A.D. McCoy, M. Ibsen, P. Horak, B.C. Thomsen, D.J. Richardson, Feasibility study of SOA-based noise suppression for spectral amplitude coded OCDMA, *J. Lightw. Technol.* 25 (January (1)) (2007) 394–401.
- [14] J. Penon, W. Mathlouthi, L.A. Rusch, S. LaRochelle, An innovative receiver for incoherent SAC-OCDMA enabling SOA-based noise cleaning experimental validation, *J. Lightw. Technol.* 27 (January (2)) (2009) 108–116.
- [15] A.M. Alhassan, N.M. Saad, N. Badruddin, An enhanced detection technique for spectral amplitude coding optical CDMA systems, *IEEE Photon. Technol. Lett.* 23 (July (13)) (2011) 875–877.
- [16] M. Abtahi, S. Ayotte, J. Penon, L.A. Rusch, Balanced detection of correlated incoherent signals: a statistical analysis of intensity noise with experimental validation, *J. Lightw. Technol.* 26 (January (10)) (2008) 1330–1338.
- [17] C.C. Yang, J.F. Huang, S.P. Tseng, Optical CDMA network codecs structured with M-sequence codes over waveguide-grating routers, *IEEE Photon. Technol. Lett.* 16 (February (2)) (2004) 641–643.
- [18] M. Rochette, S. Ayotte, L.A. Rusch, Analysis of the spectral efficiency of frequency-encoded OCDMA systems with incoherent sources, *J. Lightw. Technol.* 23 (April (4)) (2005) 1610–1619.
- [19] J.W. Goodman, *Statistical Optics*, Wiley, New York, 2000 (Chapter 6).
- [20] S. Ayotte, M. Rochette, J. Magné, L.A. Rusch, S. LaRochelle, Experimental verification and capacity prediction of FE-OCDMA using superimposed FBG, *J. Lightw. Technol.* 25 (February (2)) (2005) 724–731.